GD3 glycosphingolipid contributes to Fas-mediated apoptosis via association with ezrin cytoskeletal protein

Anna Maria Giammarioli[a,1], Tina Garofalo[b,1], Maurizio Sorice[b], Roberta Misasi[b], Lucrezia Gambardella[a], Roberto Gradini[b], Stefano Fais[c], Antonio Pavan[d], Walter Malorni[a,*]

[a] *Department of Ultrastructures, Istituto Superiore di Sanità, Viale Regina Elena 299, 00161 Rome, Italy*
[b] *Department of Experimental Medicine and Pathology, University of Rome 'La Sapienza', Rome, Italy*
[c] *Department of Immunology, Istituto Superiore di Sanità, Viale Regina Elena 299, 00161 Rome, Italy*
[d] *Department of Experimental Medicine, University of L'Aquila, L'Aquila, Italy*

Received 15 May 2001; revised 31 July 2001; accepted 1 August 2001

First published online 3 September 2001

Edited by Veli-Pekka Lehto

Abstract Efficiency of Fas-mediated apoptosis of lymphoid cells is regulated, among other means, by a mechanism involving its association with ezrin, a cytoskeletal protein belonging to the 4.1 family of proteins. In the present work, we provide evidence for a further molecule that associates to ezrin in Fas-triggered apoptosis, the disialoganglioside GD3. In fact, as an early event, GD3 redistributed in membrane-associated domains in uropods and co-localized with ezrin. Co-immunoprecipitation analyses confirmed this result, indicating a GD3–ezrin association. Altogether, these results are suggestive for a role of GD3 in Fas/ezrin-mediated apoptosis, supporting the view that uropods contain a multimolecular signaling complex involved in Fas-mediated apoptosis.

Key words: GD3; Ganglioside; Apoptosis; Fas; Ezrin

1. Introduction

It was hypothesized that apoptosis could be mediated by two different pathways that, although strictly intertwined, may represent different ways to reach the same result, i.e. the death of a cell [1,2]. The first pathway (type I) is consistently exerted by those cells that follow the CD95/Fas-mediated apoptosis initiated by active caspase 8 and finally leading to an execution phase cascade. This pathway involves mitochondria only in the late phases of the apoptotic cascade. In contrast, the second pathway (type II) is the mitochondrial branch of the apoptotic pathway where this organelle might play a primary role [2]. We have recently shown [3] that human T cells, that are susceptible to Fas-mediated apoptosis, exhibit a constitutive polarized morphology forming uropods with distinct plasma membrane domains. We also suggested that Fas polarization, through an ezrin-mediated association with the actin cytoskeleton, is a key intracellular mechanism in the regulation of Fas-mediated apoptotic signal [3].

Glycosphingolipids (GSLs), carbohydrate-bearing lipid components of biological membranes, have been implicated as mediators of cell adhesion as well as modulators of signal transduction [4]. In particular, gangliosides, sialic acid-containing GSLs, are considered to have a role as recognition sites that may mediate the interaction of the cell with its surroundings and play an important role in cell adhesion, differentiation and immune modulation [4,5]. The cell expression pattern of gangliosides depends on the cell type: in human lymphocytes, monosialoganglioside GM3 is the major ganglioside constituent [6], and disialoganglioside GD3, although in minor extent, is also well expressed [7]. Recently, we have observed that a GD3 overexpression in activated lymphocytes was strictly associated with the early events leading to cell depletion by apoptosis [8]. This increase appeared to be accompanied by qualitative changes, i.e. intracellular redistribution of GD3 molecules in typical lymphocyte structures called uropods [3,8]. Accordingly, we and others hypothesized that a portion of intracellular GD3 can play a role in apoptotic machinery [8,9]. However, although GD3 has been reported to propagate Fas-mediated apoptotic signals in myeloid tumor cells [10,11], and to be involved in mitochondrial-mediated apoptosis [9], either the mechanisms upstream of the ganglioside action and its direct targets still remain to be elucidated. On the basis of these considerations, we decided to analyze the role of GD3 in ezrin/Fas-mediated apoptosis in a human T lymphoblastoid cell line (CEM cells). The results obtained allow to hypothesize that uropods can represent a cell death key structure where a series of molecular and functional associations, i.e. of death-related molecules Fas, ezrin and GD3, probably have to take place.

2. Materials and methods

2.1. Cells

Human lymphoblastoid CEM cells were cultured in RPMI 1640 (Gibco-BRL, Life Technologies Italia srl, Milan, Italy) containing 10% fetal calf serum at 37°C in a humidified 5% CO_2 atmosphere.

2.2. Induction of apoptosis

Anti-human CD95 treatment: 250 ng/ml of an anti-human IgM mAb (clone CH11, Upstate Biotechnology, Lake Placid, NY, USA) was added to CEM cell cultures (5×10^5 cells/ml) for different time periods (10 min, 3 h, 4 h, 6 h). After treatment, cells were collected, washed and analyzed for apoptosis. Staurosporine (STS) treatment: the protein kinase inhibitor staurosporine (Sigma Chem Co., St. Louis, MO, USA) was added to the culture medium at the final concentration of 1 μM [12]. After 4 h treatment, control and treated cells were prepared for fluorescence, scanning electron microscopy (SEM) and co-immunoprecipitation.

*Corresponding author. Fax: (39)-6-49387140.
E-mail address: malorni@iss.it (W. Malorni).

[1] These authors contributed equally to this work and should thus be considered as first authors.

PII: S0014-5793(01)02776-4

2.3. Cytochalasin D (CD) treatment

Control and treated cells were exposed to CD (Sigma) before different apoptotic inducers. The CD concentration used in this study (0.5 μg/ml) inhibits actin polymerization without being cytotoxic, as assessed by analytical cytology analyses [13].

2.4. SEM analysis

CEM cells were fixed with 2.5% (v/v) glutaraldehyde in 0.1% cacodylate buffer (pH 7.4) and processed as previously described [14]. Samples were then examined with a Cambridge 360 SEM.

2.5. Immunofluorescence and intensified video microscopy (IVM)

Control and treated cells were collected by centrifugation, allowed to attach to glass coverslips pre-coated with polylysine and fixed with 4% paraformaldehyde in phosphate-buffered saline (PBS) for 30 min at room temperature. After washing in the same buffer, the cells were permeabilized with 0.5% Triton X-100 in PBS for 5 min at room temperature. For localization of CD95 and ezrin, samples were incubated at 37° for 30 min with polyclonal antibodies to CD95 (Santa Cruz Biotechnology, CA, USA) or monoclonal antibodies to ezrin, (Transduction Laboratories, Lexington, KY, USA). Cells were then incubated with TRITC-conjugated anti-rabbit IgG (Sigma) or FITC-conjugated anti-mouse IgG (Sigma) for detection of CD95 and ezrin proteins, respectively. Alternatively, the cells were incubated with GMR2 anti-GD3 mAb [8,15], a gift from Dr. T. Tai, Tokyo Metropolitan Institute of Medical Science, Tokyo, Japan, for 1 h at 37°C. This antibody showed highly restricted binding specificity, reacting only with the immunizing ganglioside. None of other gangliosides or neutral glycolipids were recognized [15]. This incubation was followed by the addition of FITC-conjugated anti-mouse IgM (Sigma) for 30 min at 37°C. After washing, all samples were mounted with glycerol–PBS (2:1) and observed with a Nikon Microphot fluorescence microscope. IVM images were obtained by a chilled color 3CCD camera (Hamamatsu, Japan). Normalization and background subtraction were performed for each image. Figures were obtained by the OPTILAB (Graftek, France) software for image analysis.

2.6. Scanning confocal microscopy

Anti-CD95-treated and untreated CEM cells were fixed as reported above, or alternatively, incubated in the presence of acetone–methanol 1:1 (v/v) for 10 min at 4°C and then soaked in balanced salt solution (Sigma) for 30 min at room temperature. Cells were then labeled with anti-GD3 mAb for 1 h at 4°C, followed by addition with FITC-conjugated goat anti-mouse IgM (Sigma) for 45 min at 4°C. After washing with PBS at 4°C, cells were then counterstained with monoclonal antibody to ezrin (Biogenesis, UK), followed by the addition of Texas red-conjugated anti-mouse IgG (Sigma) for 30 min at 4°C. The cellular distribution of GD3 molecules was analyzed by scanning confocal microscopy. Images were acquired through a laser scanning confocal microscope Zeiss LSM 510 (Zeiss, Oberkochen, Germany) equipped with argon and HeNe ion lasers. Simultaneously, the green (FITC) and the red (Texas red) fluorophores were excited at 488 and 518 nm and were observed by two different detectors. Images were collected at 1024×1024 pixels.

2.7. Evaluation of apoptosis

Apoptosis was evaluated by morphometric analyses and by flow cytometry. To assess nuclear morphology, cells fixed in paraformaldehyde, were dyed with Hoechst 33258 (10 μg/ml) for 30 min at 37°C. Slides were rinsed in PBS and mounted with glycerol–PBS (2:1) and observed with a Nikon Microphot fluorescence microscope. Quantitative evaluation of apoptotic cells was performed by counting at least 300 cells at a 50× magnification. DNA fragmentation was studied by propidium iodide (PI) staining followed by flow cytometric analysis (EPICS Profile, Coulter Electronics, Hialeah, FL, USA). Cells were fixed with cold 70% ethanol in PBS for 1 h at 4°C. After centrifugation at 200×*g* for 10 min at 4°C, cells were washed once in PBS. The pellet was resuspended in 0.5 ml PBS, 50 μl of RNAse (type I-A; Sigma; 10 mg/ml in PBS) was added, followed by 1 ml PI (Sigma; 100 μg/ml in PBS) solution. The cells were incubated in the dark at room temperature for 15 min and kept at 4°C in the dark until measured. A Trypan blue exclusion test was performed to evaluate the viability of the cultures.

2.8. Co-immunoprecipitation and high-performance thin-layer chromatography (HPTLC) analysis of ganglioside extracts

GD3–protein association was analyzed by co-immunoprecipitation as described [16]. Briefly, first, anti-CD95-treated, STS-treated or untreated CEM cells were lysed in lysis buffer (20 mM HEPES, pH 7.2, 1% Nonidet P-40, 10% glycerol, 50 mM NaF, 1 mM phenylmethylsulfonyl fluoride, 10 μg of leupeptin per ml). Then, cell-free lysates were mixed with protein G-acrylic beads and stirred by a rotary shaker for 2 h at 4°C to pre-clear non-specific binding. After centrifugation (500×*g* for 1 min), the cleared supernatant was immunoprecipitated with anti-ezrin mAb (Biogenesis, UK) plus protein G-acrylic beads. As a negative control, a mouse IgG with irrelevant specificity (Sigma) was employed. The immunoprecipitates were then subjected to ganglioside extraction, according to the method of Svennerholm and Fredman [17], with minor modifications. Briefly, immunoprecipitates were extracted twice in chloroform:methanol:water (4:8:3, v/v) and subjected to Folch partition by the addition of water to give a final chloroform:methanol:water ratio of 1:2:1.4. The upper phase, containing polar GSLs, was desalted and low molecular weight contaminants were removed using Supelclean LC-18 tubes (Supelco Inc., Bellefonte, PA, USA), according to the method of Williams and McCluer [18]. The eluted GSLs were dried and separated by HPTLC, using silica gel 60 HPTLC plates (Merck, Darmstadt, Germany). Chromatography was performed in chloroform:methanol:0.25% aqueous KCl (5:4:1, v:v). Plates were air-dried and gangliosides visualized with resorcinol [19]. Densitometric scanning analysis was performed by Mac OS 9.0 (Apple Computer International), using NIH Image 1.62 software.

To identify ganglioside molecule(s) co-migrating with GD3, TLC immunostaining was performed on aluminum-backed silica gel plates (Merck, Darmstadt, Germany), as previously described [20], using the anti-GD3 mAb GMR2 [15].

In order to verify the immunoprecipitation of ezrin molecules, a portion of the immunoprecipitates was run on 10% SDS–PAGE and then probed with polyclonal anti-ezrin Ab (Santa Cruz Biotech Inc., Santa Cruz, CA, USA). Bound antibodies were then visualized with peroxidase-conjugated anti-goat IgG (Sigma), and immunoreactivity assessed by chemiluminescence reaction using the ECL Western blocking detection system (Amersham, Buckinghamshire, UK).

3. Results

3.1. Fas, ezrin and GD3 polarization in uropod-forming cells

We first evaluated the cellular distribution of Fas, ezrin and GD3 molecules in CEM lymphoblastoid cells by immunofluorescence microscopy. We found that both Fas and ezrin (Fig. 1a,b) were mainly observable as plasma-membrane-associated domains in the apical portion of uropods of CEM cells which, by SEM analyses, appeared as large bulbs forming long cell protrusions (Fig. 1c). By contrast, the anti-GD3 signal, after Triton X-100 extraction, appeared as a punctate positivity throughout the cell cytoplasm including uropods (Fig. 1d). When experiments on CD95/Fas-mediated apoptotic triggering were carried out, a rearrangement of GD3 distribution was detected by IVM observations. In fact, ganglioside molecules were mainly found in the uropod (Fig. 1e). Moreover, this redistribution appeared to depend upon the integrity of actin filament network. In fact, when cells were pre-treated with CD, an inhibitor of actin polymerization used at low, non-cytotoxic concentrations [3], an inhibition of apoptosis as well as no sign of GD3 polarization were detected (Fig. 1f).

3.2. GD3 distribution in uropod-forming cells

Since apoptosis is a 'dynamic' process, we decided to evaluate the time-course of the above described phenomena. In particular, GD3 analytical cytology studies were carried out at different times after anti-Fas treatment (up to 4 h). Fig. 2 shows the progressive rearrangement and redistribution of

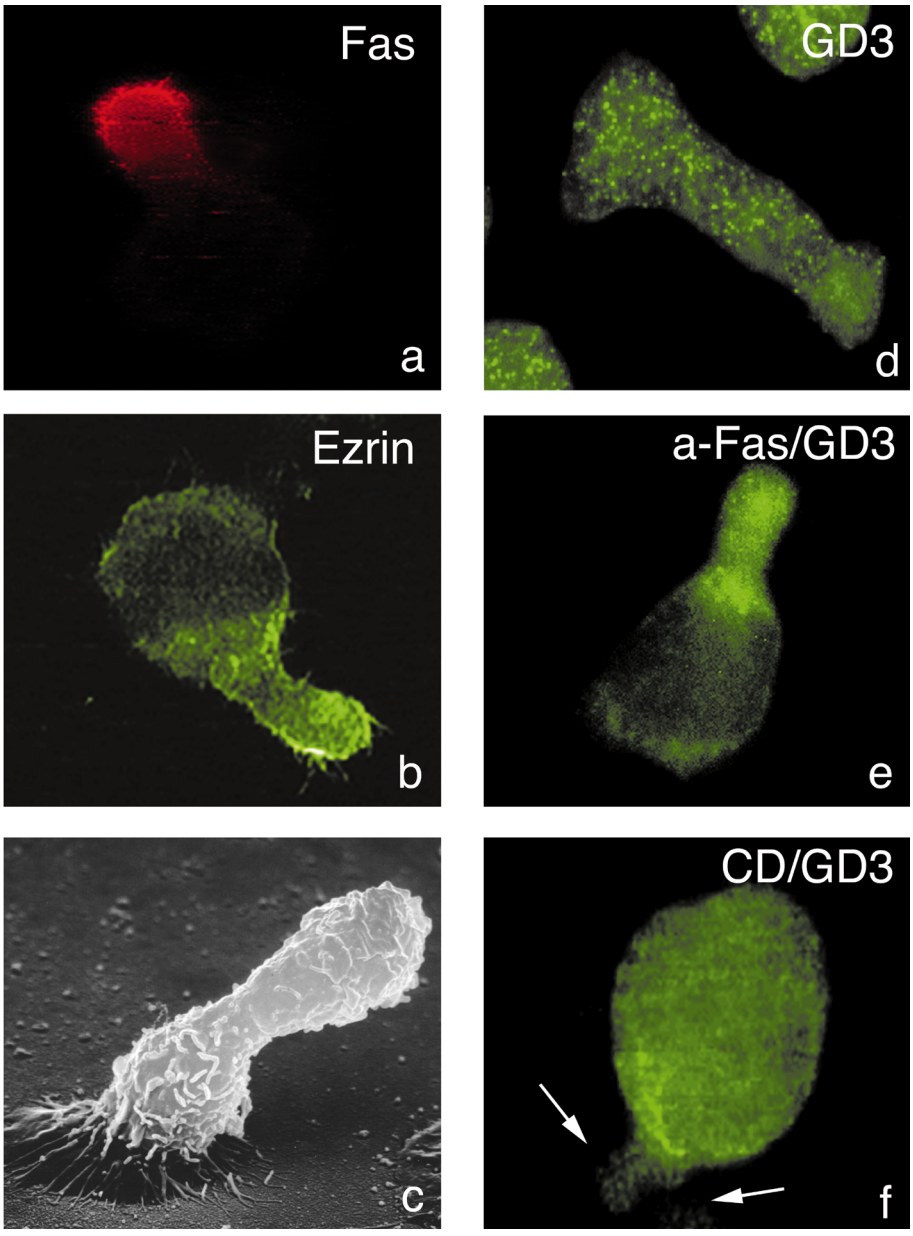

Fig. 1. IVM of CEM cells. The presence of Fas (a) as well as ezrin (b) molecules in the uropod of CEM cells is well visible. A SEM micrograph displaying ultrastructural features of a typical uropod is shown in (c). GD3 molecules appear randomly distributed in the cell, including uropod of Triton-permeated cells (d). Fas treatment induced an increased presence of GD3 in the uropod (e). After cytochalasin B treatment, the uropod appears as a GD3-negative structure (f, arrows indicate the uropod). Magnification 1716×.

GD3 molecules forming clumps towards the cell periphery (Fig. 2a–c). After 4 h, the ganglioside staining is mainly detected in the uropods (Fig. 2d). Notably, apoptosis evaluation clearly indicated that Fas-mediated apoptosis in our experimental conditions led to high rates of cell death only after 4–6 h (Fig. 2g). Hence, redistribution of GD3 appeared to occur as an early event. Finally, in consideration of the different mechanisms employed by various apoptotic stimuli, the effects of a different apoptotic inducer, i.e. STS, was also assessed. This drug is in fact targeted to mitochondria and, unlike Fas (type I), it is considered as a typical type II inducer [2]. In this case no rearrangement of GD3 was detected (Fig. 2f).

3.3. GD3–ezrin co-localization in Fas-triggered CEM cells

To investigate whether GD3 and ezrin polarization resulted in a direct interaction within specific domains of CEM cells, we analyzed their distribution by scanning confocal microscopy and superimposed the double-immunostaining patterns obtained by using anti-GD3 and anti-ezrin antibodies. Our results showed that in cells incubated with anti-CD95/Fas for 4 h, the GD3 signal appeared localized on the cell surface and intracellularly, resembling specific cytoplasmic compartment(s). The anti-GD3 staining appeared mainly confined to the uropods (Fig. 3a,e). In the same cells, the anti-ezrin staining was also present within uropods (Fig. 3b,f). Merging of the images of anti-GD3 and anti-ezrin staining showed a nearly complete overlap, as indicated by the yellow areas. This indicates that ezrin molecules were localized in cell protrusions (uropods) enriched with GD3 molecules (Fig. 3c,d,g,h).

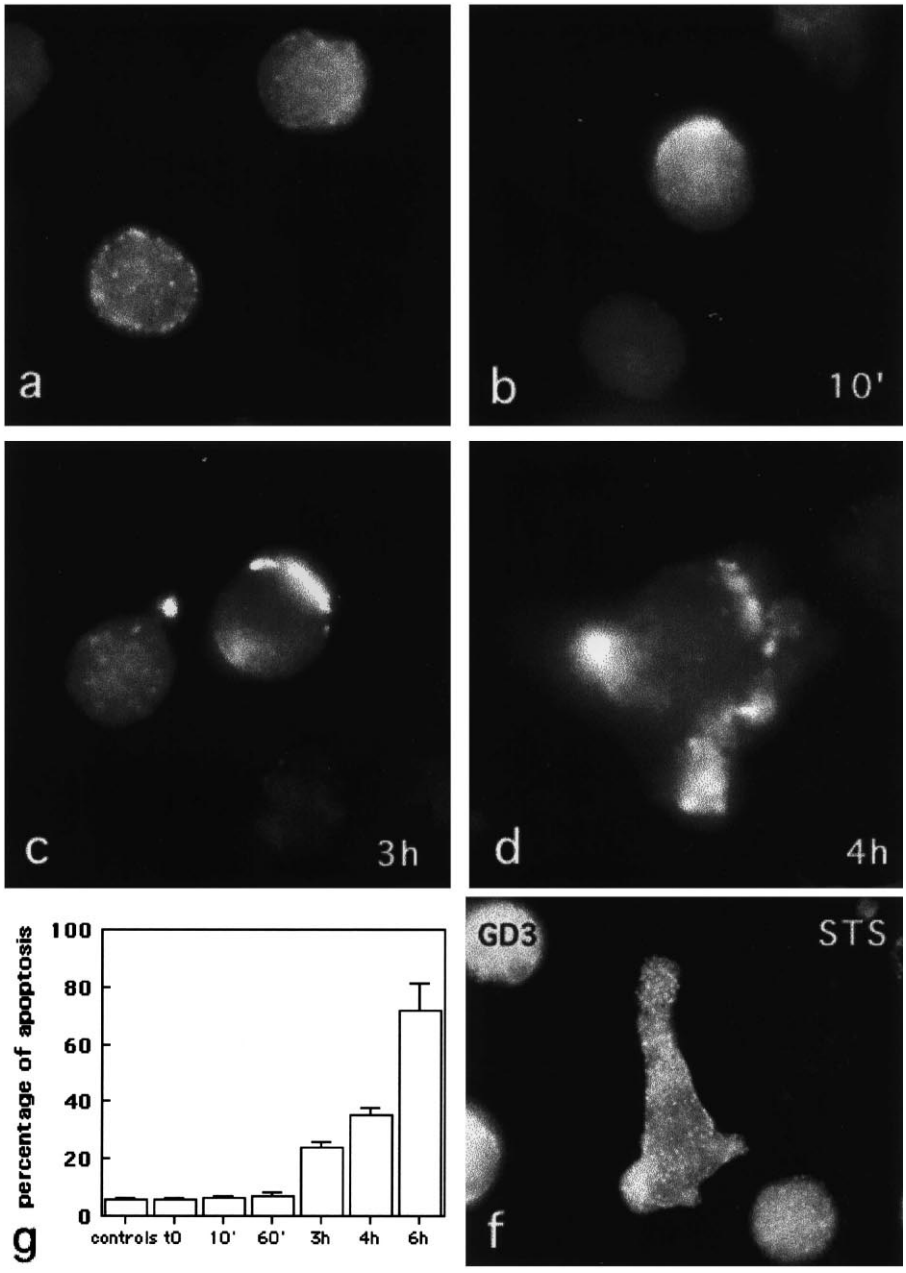

Fig. 2. IVM of Fas-treated CEM cells. Time-course analysis indicating the time-dependent redistribution of GD3 in the uropods (a–d). Note that the presence of GD3 in the uropods appears to be related to the increased apoptotic ratio found after 4 h of Fas exposure (g). STS apoptotic stimulus exposure did not induce GD3 redistribution (f).

3.4. GD3 co-immunoprecipitates with ezrin in FAS-triggered CEM cells

To verify whether GD3 binds directly to ezrin, cell-free lysates from anti-Fas-treated and untreated CEM cells were immunoprecipitated with the anti-ezrin mAb, followed by protein G-acrylic beads. Acidic GSLs were then extracted from the ezrin immunoprecipitates. They were then analyzed by and HPTLC, which showed a disialoganglioside GD3 co-migrating band in the extracts from anti-Fas-treated cells (4 h) (Fig. 4, lane a). A tiny band co-migrating with GM3 was also observed, suggesting the presence of a small amount of GM3. The GM3 double band is due to the heterogeneity of fatty acid composition. In these cells (treated with anti-Fas for 4 h) we observed: (i) GD3 content in the immunoprecipitate was 2.42-fold as compared to GM3, as detected by densitometric analysis (Fig. 4); (ii) the total content of the two gangliosides was about 4 μg of GM3/10^8 and 0.4 μg of GD3/10^8 cells, as detected by measuring the lipid-bound sialic acid. Thus, GD3 resulted in about 24-fold enriched in the ezrin immunoprecipitates in comparison to GM3. No resorcinol-positive bands were detectable in the immunoprecipitates from cells treated with anti-Fas for 10 min (Fig. 4, lane b), cells treated with STS (Fig. 4, lane c), or in untreated cell extracts (Fig. 4, lane d). In control samples, the immunoprecipitation with a mouse IgG, with irrelevant specificity, under the same conditions did not result in detectable levels of GD3 or GM3 (Fig. 4, lane e). The identity of GD3 was confirmed by immunostaining on TLC of the immunoprecipitates with the GMR2 mAb (Fig.

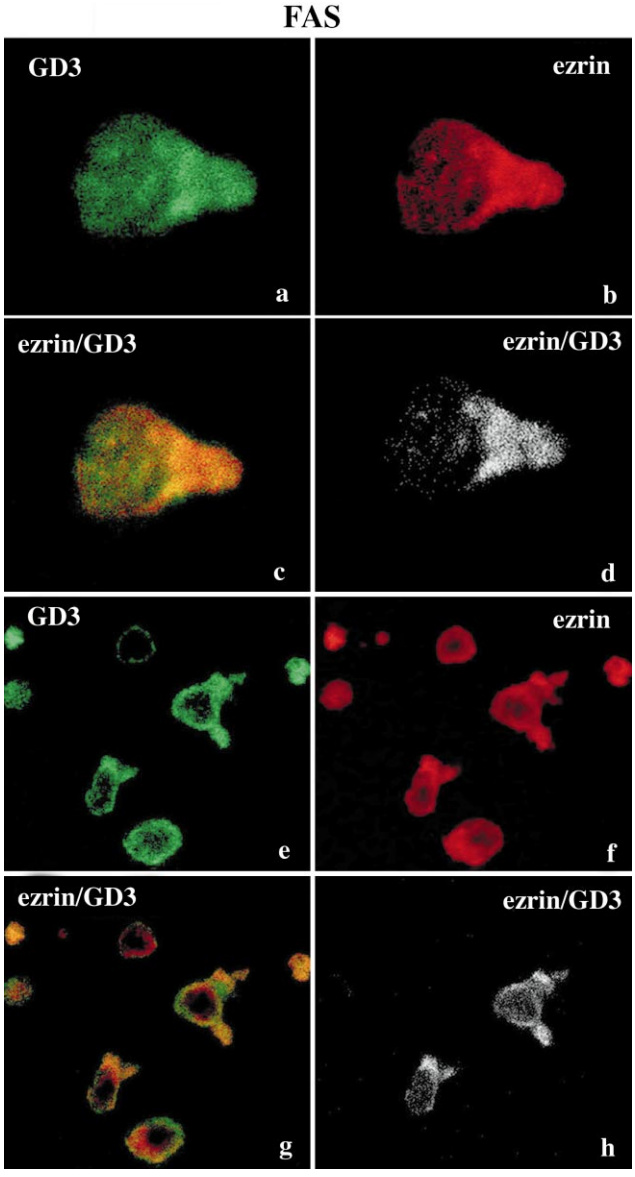

Fig. 3. Scanning confocal microscopic analysis of GD3–ezrin association on a CEM plasma membrane after anti-CD95/Fas treatment. Cells were labeled with anti-GD3 mAb (GMR2), followed by the addition of FITC-conjugated anti-mouse IgM. Cells were then incubated with anti-ezrin, followed by the addition of Texas red-conjugated anti-mouse IgG. Magnification 1072× (pictures a–d); 512× (pictures e–h). Fas treatment clearly induced a redistribution of GD3 (a,e) and ezrin (b,f) within uropods; anti-GD3 and anti-ezrin double-staining revealed yellow areas, corresponding to nearly complete co-localization (c,g); dual immunofluorescence image analysis represents exclusively the co-localization areas of GD3–ezrin (d,h).

4, lane g). Again, no anti-GD3-positive bands were detectable in untreated cell extracts (Fig. 4, lane h).

4. Discussion

Mechanisms of apoptosis have recently been investigated by several works trying to point out the cascade of events that follows apoptotic triggering. In the present study we show, for the first time, that in type I, Fas-mediated apoptosis, GD3 ganglioside associates to ezrin cytoskeleton, suggesting its possible role in the very early steps of apoptotic cascade and prior to the subsequent, late mitochondrial-mediated events [2,21]. Thus, our indications of a further activity of GD3 in apoptosis machinery are in agreement with previously reported data regarding target activity of GD3 on mitochondria [9].

It was demonstrated that either pharmacological inhibition of GD3 synthesis or cell exposure to GD3 synthase antisense oligodeoxynucleotides prevented CD95/Fas-mediated apoptosis [10]. On the other hand, ezrin antisense oligonucleotides hindered Fas-mediated apoptosis, indicating the requirement of actin-cytoskeleton integrity and function in the Fas-mediated cascade leading to cell death [3]. It was also hypothesized that GD3 ganglioside could mediate the 'propagation' of Fas-generated pro-apoptotic signals [10]. Hence, in light of the results reported herein, we can hypothesize that this mediation could occur by a structural association of GD3 with ezrin molecules. Specific high-affinity SDS-resistant ganglioside–protein interactions reported in different cell types appear in fact to be involved in transducing stimulatory and/or inhibitory cellular signals [22,23]. In addition, we cannot rule out the possibility that other 4.1 family molecules, e.g. moesin or radixin, could be similarly involved. It can also be hypothesized that ezrin–GD3 molecular association can represent a prerequisite for ganglioside cytoplasmic trafficking, and that it can finally lead to the mitochondrial effects previously described in literature [9]. In fact, on the basis of our results (see Fig. 1d) and literature data [5], the presence of gangliosides in several subcellular structures can be taken into account. Moreover, changes of ganglioside distribution in the cell cytoplasm have been suggested to be regulated by various cytoskeleton elements [24]. Accordingly, low concentrations of microfilament perturbating agent CD not only impaired Fas-mediated apoptosis cascade [2], but, as shown herein, also affected GD3 molecule distribution. Hence, altogether, these findings seem to suggest that the scattered distribution of GD3-associated Triton-insoluble domains found in control CEM cells can be modified by CD95/Fas stimulation via an ezrin association. This could also suggest that association with cytoskeleton can play a key role in cytoplasmic movements of GD3 molecule finally targeted to mitochondria [9] and leading to apoptosis.

On the other hand, a typical mitochondrially targeted drug, such as STS, capable of directly acting on mitochondrial membrane transition in CEM cells [25] induced neither GD3 redistribution nor GD3–ezrin association. Hence, although several experiments have to be performed to better elucidate this point, e.g. by using ezrin antisense oligonucleotides (manuscript in preparation), we cannot rule out a specific activity of ezrin molecules in the efficiency of earlier steps of Fas-mediated cell death signaling via its association with GD3 gangliosides. Indeed, co-immunoprecipitation experiments revealed the presence of GD3 and GM3 molecules in the ezrin immunoprecipitate. This finding, together with scanning confocal microscopic analyses, strongly suggest that Fas-triggered apoptosis induces ezrin association with plasma-membrane raft microdomains. This hypothesis is in agreement with previously suggested links between raft-mediated signaling and the interaction of actin cytoskeleton with membrane raft domains [26] and the possible role of 4.1 family proteins ezrin and moesin in redistribution and trafficking of other important molecules in the uropods of T lymphocytes [27].

Altogether, our findings represent the first evidence of an association between GD3 ganglioside and ezrin molecules

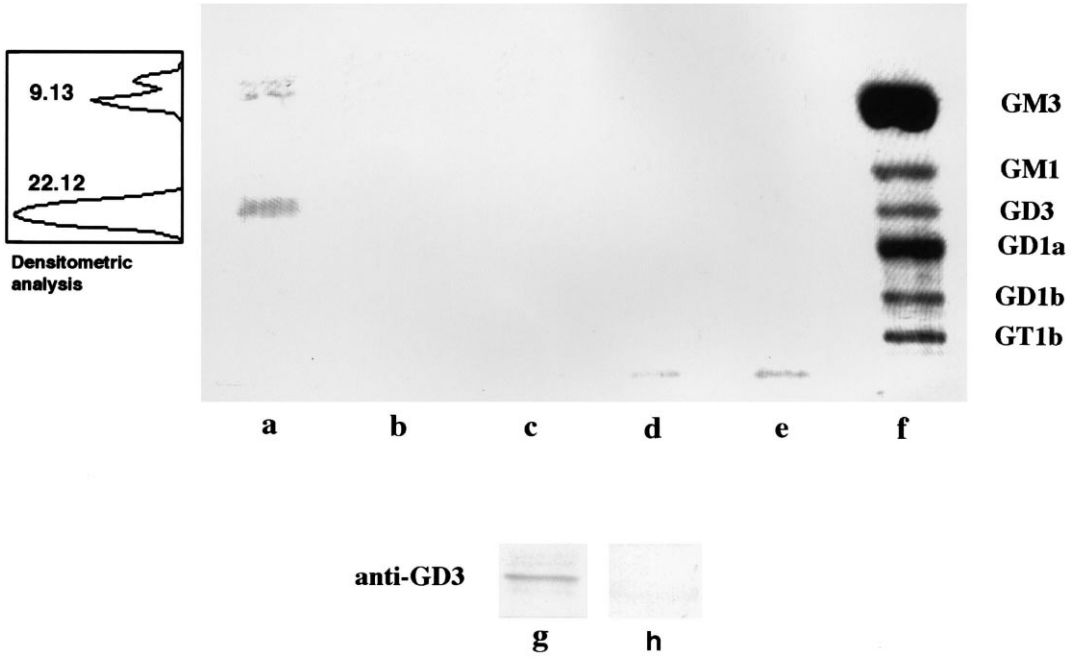

Fig. 4. HPTLC analysis of ganglioside pattern of ezrin immunoprecipitates. Anti-Fas-treated and untreated cells were lysed in lysis buffer. Cell-free lysates were immunoprecipitated with anti-ezrin mAb. Lane a: gangliosides extracted from ezrin immunoprecipitate after anti-Fas treatment (4 h). A GD3 co-migrating band is clearly evident; a tiny GM3 co-migrating band is also detectable. Densitometric scanning analysis shows the intensity of the GD3 and GM3 co-migrating bands detected in ezrin immunoprecipitate after anti-Fas treatment (4 h). Arbitrary units; lane b: gangliosides extracted from ezrin immunoprecipitate after anti-Fas treatment (10 min); lane c: gangliosides extracted from ezrin immunoprecipitate after STS treatment; lane d: gangliosides extracted from untreated ezrin immunoprecipitate; lane e: gangliosides extracted from irrelevant mouse IgG immunoprecipitate; lane f: standard gangliosides; lane g: GD3 immunostaining analysis on TLC from ezrin immunoprecipitates of anti-Fas-treated cells; lane h: GD3 immunostaining analysis on TLC from ezrin immunoprecipitates of untreated cells.

after Fas triggering, suggesting that membrane raft microdomains mediate lateral assemblies involved in Fas-mediated apoptosis. This could also be of relevance in the understanding of the mechanisms of regulation of this cell death process [9] in terms of both resistance and susceptibility.

References

[1] Dragovich, T., Rudin, C.M. and Thompson, C.B. (1998) Oncogene 17, 3207–3213.
[2] Schmitz, I., Walczak, H., Krammer, P.H. and Peter, M.E. (1999) Cell Death Differ. 6, 821–822.
[3] Parlato, S., Giammarioli, A.M., Logozzi, M., Lozupone, F., Matarrese, P., Luciani, F., Falchi, M., Malorni, W. and Fais, S. (2000) EMBO J. 19, 5123–5134.
[4] Hakomori, S. (2000) Glycoconjug. J. 17, 143–151.
[5] Garofalo, T., Sorice, M., Misasi, R., Cinque, B., Giammatteo, M., Pontieri, G.M., Cifone, M.G. and Pavan, A. (1998) J. Biol. Chem. 273, 35153–35160.
[6] Kiguchi, K., Henning-Chubb, B.C. and Huberman, E. (1990) J. Biochem. 107, 8–14.
[7] Merrit, W.D., Taylor, B.J., Der-Minassian, V. and Reaman, G.H. (1996) Cell. Immunol. 173, 131–148.
[8] Misasi, R., Sorice, M., Garofalo, T., Griggi, T., Giammarioli, A.M., d'Ettorre, G., Vullo, V., Pontieri, G.M., Malorni, W. and Pavan, A. (2000) AIDS Res. Hum. Retroviruses 16, 1539–1549.
[9] Rippo, M.R., Malisan, F., Ravagnan, L., Tomassini, B., Condo, I., Costantini, P., Susin, S.A., Rufini, A., Todaro, M., Kroemer, G. and Testi, R. (2000) FASEB J. 14, 2047–2054.
[10] De Maria, R., Lenti, L., Malisan, F., d'Agostino, F., Tomassini, B., Zeuner, A., Rippo, M.R. and Testi, R. (1997) Science 277, 1652–1655.
[11] De Maria, R., Rippo, M.R., Schuchman, E.H. and Testi, R. (1998) J. Exp. Med. 187, 897–902.
[12] Eischen, C.M., Kottke, T.J., Martins, L.M., Basi, G.S., Tung, J.S., Earnshaw, W.C., Leibson, P.J. and Kaufmann, S.H. (1997) Blood 90, 935–943.
[13] Cooper, J.A. (1987) J. Cell Biol. 105, 1473–1478.
[14] Malorni, W., Iosi, F., Santini, M.T. and Testa, U. (1993) J. Cell Sci. 106, 309–318.
[15] Ozawa, H., Kotani, M., Kawashima, I. and Tai, T. (1992) Biochim. Biophys. Acta 1123, 184–190.
[16] Iwabuchi, K., Handa, K. and Hakomori, S.I. (2000) Methods Enzymol. 312, 488–494.
[17] Svennerholm, L. and Fredman, P.A. (1980) Biochim. Biophys. Acta 617, 97–109.
[18] Williams, M.A. and McCluer, R.H. (1980) J. Neurochem. 35, 266–269.
[19] Svennerholm, L. (1957) Biochim. Biophys. Acta 24, 604–611.
[20] Misasi, R., Sorice, M., Griggi, T., d'Agostino, F., Garofalo, T., Masala, C., Pontieri, G.M. and Lenti, L. (1993) Clin. Immunol. Immunopathol. 67, 216–223.
[21] Kroemer, G., Zamzami, N. and Susin, S.A. (1997) Immunol. Today 18, 44–51.
[22] Mutoh, T., Tokuda, A., Miyadai, Y., Hamaguchi, M. and Fujiki, N. (1995) Proc. Natl. Acad. Sci. USA 92, 5087–5091.
[23] Hakomori, S., Handa, K., Iwabuchi, K., Yamamura, S. and Prinetti, A. (1998) Glycobiology 8, XI–XIX.
[24] Fentie, I.H. and Roisen, F.J. (1993) J. Neurocytol. 22, 498–506.
[25] Matarrese, P., Testa, U., Cauda, R., Vella, S., Gambardella, L. and Malorni, W. (2001) Biochem. J. 355, 587–595.
[26] Harder, T. and Simons, K. (1999) Eur. J. Immunol. 29, 556–562.
[27] Serrador, J.M., Nieto, M., Alfonso-Lebrero, J.L., del Pozo, M.A., Calvo, J., Furthmayr, H., Schwartz-Albiez, R., Lozano, F., Gonzales-Amaro, R., Sanches-Mateos, P. and Sanchez-Madrid, F. (1998) Blood 91, 4632–4644.